

## Kondo effect and impurity band conduction in Co:TiO<sub>2</sub> magnetic semiconductor

R. Ramaneti, J. C. Lodder, and R. Jansen

MESA<sup>+</sup> Institute for Nanotechnology, University of Twente, 7500 AE Enschede, The Netherlands

(Received 29 July 2007; published 26 November 2007)

The nature of charge carriers and their interaction with local magnetic moments in an oxide magnetic semiconductor is established. For cobalt-doped anatase TiO<sub>2</sub> films, we demonstrate conduction in a metallic donor-impurity band. Moreover, we observe a clear signature of the Kondo effect in electrical transport data with remarkably high Kondo temperatures of up to 120 K. This indicates a strong coupling between local Co moments and delocalized electrons in the impurity band.

DOI: [10.1103/PhysRevB.76.195207](https://doi.org/10.1103/PhysRevB.76.195207)

PACS number(s): 85.75.-d, 72.25.Dc, 75.47.-m, 75.50.Pp

Ferromagnetic semiconductors (FMSCs) are an intriguing novel class of materials in which magnetic ions are introduced into a semiconductor at dilute concentrations that preclude a direct exchange interaction.<sup>1,2</sup> Nevertheless, strong ferromagnetic interactions are found, which for GaMnAs, the archetypal FMSC, were shown to be mediated by *delocalized carriers* (holes). This leads to remarkable properties such as a ferromagnetic coupling and a macroscopic magnetization that depends on the carrier density, allowing electric field control of magnetism.<sup>3</sup> Unfortunately, the Curie temperature of GaMnAs is so far limited to 170 K. Hence, the development of other FMSC materials is a key objective in the quest for novel (spin-) electronic devices<sup>4</sup> that employ the spin degree of freedom and operate at room temperature. Recent reports<sup>5-7</sup> of room temperature ferromagnetism in Co:TiO<sub>2</sub> films have therefore spurred intense research activities. Ferromagnetism has now been observed in numerous conducting oxide semiconductors including TiO<sub>2</sub>, ZnO, SnO<sub>2</sub>, and In<sub>2</sub>O<sub>3</sub> doped with various transition metal ions,<sup>5-14</sup> and with surprisingly high magnetic ordering temperature [up to 930 K (Ref. 13)]. However, whether ferromagnetism in doped oxide FMSC is intrinsic and derives from a common carrier mediated interaction is still unclear.

Several studies of doped oxide FMSC have focused on magnetic, structural, and chemical properties. Yet, charge carriers are thought to be crucial to the magnetism in FMSC, while technological interest derives from the unique prospects for applications in novel spin-transport devices. The key issues are therefore to establish whether the room temperature ferromagnetism is intrinsic and carrier mediated and to establish whether the carriers are spin polarized. This, in turn, is determined by the nature of the charge carriers and their coupling to the magnetic dopants. The coupling can result in a net ferromagnetic interaction between different magnetic dopants, for which two models have been proposed: (i) a Ruderman-Kittel-Kasuya-Yosida (RKKY) type of magnetic coupling mediated by free carriers in the valence or conduction band of the host semiconductor,<sup>2</sup> and (ii) exchange interaction between magnetic ions and a metallic donor-impurity band.<sup>12</sup> The latter can be derived from shallow donors at sufficiently large concentration such that their hydrogenlike orbitals (with Bohr radius  $r_H$ ) overlap and carriers become delocalized.<sup>15</sup> It is clear that in order to develop a correct theoretical description of the high-temperature ferromagnetism in FMSC, it is essential to determine the nature of the carriers. This has been widely discussed for GaMnAs,

for which the importance of impurity band conduction was recently emphasized.<sup>16</sup> It is also essential to determine whether there is interaction between the carriers and the magnetic moments in the system. To examine that, we use here the Kondo effect<sup>17</sup> arising from the resonant interaction between the conduction electrons and a local spin. While it does not lead to ferromagnetism and is usually associated with metallic systems or quantum dots,<sup>18</sup> it allows one to examine whether the conduction electrons and local moments are in states that are energetically close enough to have interaction, while the magnitude of the Kondo effect provides information about the interaction strength. Neither the impurity band conduction nor the Kondo effect has hitherto been observed in oxide magnetic semiconductors.

Thus, we examine here electrical transport in anatase Co:TiO<sub>2</sub> ferromagnetic semiconductor films. We establish the nature of the charge carriers and provide the first conclusive experimental evidence for a metallic impurity band with delocalized carriers in an oxide FMSC. In addition, we present electrical transport data that show a clear signature of the Kondo effect,<sup>17</sup> directly establishing interaction between conduction electrons and Co local moments. We find remarkably high Kondo temperatures up to 120 K, indicating a strong interaction.

The films were grown by pulsed laser deposition (PLD) on TiO<sub>2</sub> terminated SrTiO<sub>3</sub>(100) substrates at a temperature of 550 °C using a Ti<sub>1-x</sub>Co<sub>x</sub>O<sub>2</sub> target with  $x=0.014$ . The oxygen pressure  $P_{ox}$  during growth, target-substrate distance, and laser repetition rate were varied. X-ray diffraction shows that films are purely anatase TiO<sub>2</sub> up to a thickness of 200 nm, with only anatase (004) and (008) reflections detectable. This was confirmed by transmission electron microscopy analysis,<sup>19</sup> which for our instrument is capable of detecting secondary phases (such as rutile TiO<sub>2</sub>) with diameter down to about 5 nm. To determine the Hall constant and carrier concentration, Hall transport data were taken with magnetic fields of up to 8.5 kOe applied perpendicular to the film plane. For the Co-doped films, this was also observed to produce a contribution from the anomalous Hall effect. However, we found<sup>19</sup> this to be much smaller than the ordinary Hall voltage, such that accurate measurements of the latter are possible over the full temperature range used here. A representative example of such Hall data on similar films can be found in Ref. 19.

Electrical transport data are shown in Fig. 1 for Co-doped

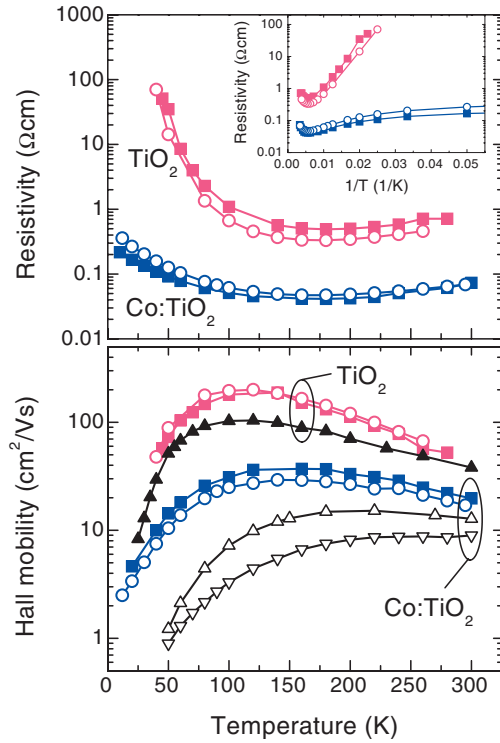


FIG. 1. (Color) Electrical properties of anatase  $\text{TiO}_2$  and  $\text{Co:TiO}_2$ . Shown are resistivity and Hall mobility versus temperature for two undoped  $\text{TiO}_2$  films (pink symbols) and two  $\text{Co:TiO}_2$  films (blue symbols) grown under the same deposition conditions (5 Hz,  $7 \times 10^{-5}$  mbar) at target-substrate distances of 48 mm (open circles) and 57 mm (solid squares). The inset shows the resistivity of these films versus  $1/T$ . The triangles show the mobility for films grown under more oxygen deficient conditions: (solid black triangles) pure  $\text{TiO}_2$ , 20 Hz,  $7 \times 10^{-5}$  mbar; ( $\Delta$ )  $\text{Co:TiO}_2$ , 5 Hz,  $3 \times 10^{-3}$  mbar; and ( $\nabla$ )  $\text{Co:TiO}_2$ , 5 Hz,  $6 \times 10^{-3}$  mbar. Film thickness is 150–200 nm.

as well as undoped, pure  $\text{TiO}_2$  films. The resistivity  $\rho$  at room temperature is  $\sim 1 \Omega \text{ cm}$  for pure  $\text{TiO}_2$  films and about an order of magnitude smaller for the Co-doped films. The low-temperature ( $T$ ) behavior of the doped films is distinctly different. As shown in the inset, for the pure  $\text{TiO}_2$  films,  $\rho$  increases exponentially with  $1/T$ , indicative of activated transport, whereas  $\rho$  of the Co-doped films remains comparatively constant and tends to saturate at low temperature. This suggests a different conduction mechanism. We confirmed that the resistivity at low  $T$  does not obey the  $\log(\rho) \propto T^{-1/2}$  relation previously reported for hopping transport in rutile samples containing Co metal clusters.<sup>20</sup> The Hall mobility, defined as  $\mu_H = R_H/\rho$ , with  $R_H$  the measured Hall constant, is strikingly lower when Co is incorporated, particularly at low  $T$  where the difference is 1 or 2 orders of magnitude (bottom panel). At 300 K, Co doping reduces the mobility only slightly to 10–20  $\text{cm}^2/\text{Vs}$ .

Information on the carrier density  $n$  is obtained from the Hall constant  $R_H = 1/ne$  (with  $e$  the electron charge) for a series of undoped  $\text{TiO}_2$  films grown at the same  $P_{ox}$  of  $7 \times 10^{-5}$  mbar, but with the laser repetition rate varied from 5 to 20 Hz (Fig. 2, top panel). For films grown at low rate (5 Hz,  $\sim 0.2 \text{ nm/s}$ ), the density of mobile carriers decreases

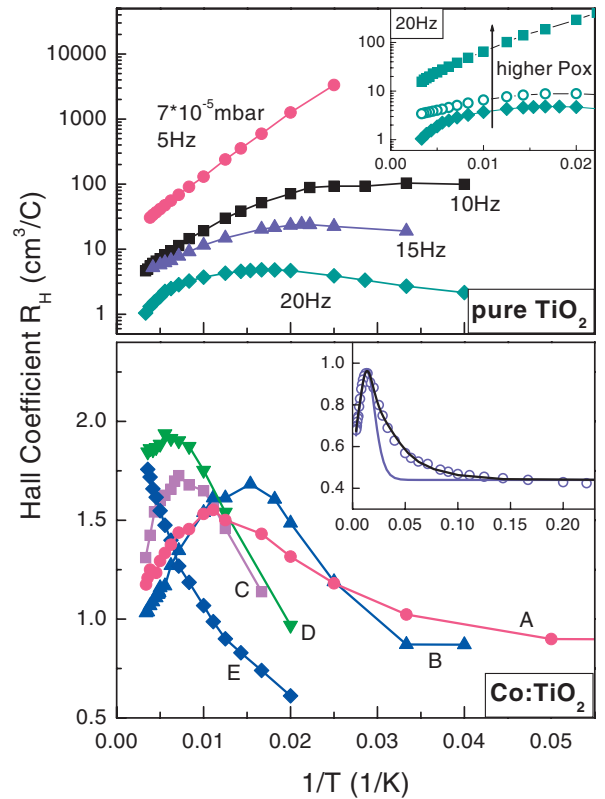


FIG. 2. (Color) Top panel: Hall constant for pure  $\text{TiO}_2$  films grown at 5–20 Hz and  $7 \times 10^{-5}$  mbar. Inset shows  $R_H$  versus  $1/T$  for films grown at 20 Hz and  $P_{ox}$  of  $7 \times 10^{-5}$ ,  $9 \times 10^{-5}$ , and  $2.5 \times 10^{-4}$  mbar. Bottom panel: Hall constant for  $\text{Co:TiO}_2$  films grown at 5 Hz and different  $P_{ox}$ : (A)  $7 \times 10^{-5}$  mbar, (B)  $5 \times 10^{-4}$  mbar, (C)  $8 \times 10^{-4}$  mbar, (D)  $2 \times 10^{-3}$  mbar, and (E)  $6 \times 10^{-3}$  mbar. Inset shows  $R_H$  vs  $1/T$  for a film grown at 20 Hz and  $7 \times 10^{-5}$  mbar, along with fits (see text). Units for insets and main panels are the same.

exponentially with  $T$ . This is expected if transport is dominated by conduction band electrons thermally activated from shallow donor-impurity levels. The activation energy  $E_A$  is 20 meV and the total carrier density  $n_0 = 5 \times 10^{17} \text{ cm}^{-3}$ . A significant change occurs when the growth rate is increased, which at constant oxygen pressure leads to more oxygen deficiency in the films. The Hall constant is reduced (and thus  $n$  increased), consistent with a larger number of shallow donors, and a maximum develops that shifts to higher  $T$  for larger growth rate. This signals a transition to impurity conduction at carrier densities above  $\sim 10^{18} \text{ cm}^{-3}$ , consistent with the Mott criterion<sup>15</sup> for carrier delocalization ( $n^{1/3}r_H > 0.25$ ) above a critical carrier concentration  $n_{crit}$ . We estimate the Bohr radius from  $r_H = \epsilon(m_e/m^*)a_0$  (with  $a_0 = 0.53 \text{ \AA}$ ) and the donor binding energy from  $E_B = (m^*/m_e) \times (R_\infty/\epsilon^2)$  (with  $R_\infty = 13.6 \text{ eV}$ ). Using the static dielectric constant  $\epsilon = 31$  and the effective mass  $m^*/m_e \approx 1.2$ , we obtain  $E_B = 17 \text{ meV}$  and  $r_H = 14 \text{ \AA}$ , which, in turn, gives  $n_{crit} \approx 6 \times 10^{18} \text{ cm}^{-3}$ , in good agreement with our transport data and previous work.<sup>21</sup> The inset of Fig. 2 shows that growth at constant rate (20 Hz) but decreasing  $P_{ox}$  has the same effect on  $R_H$  as growth at constant  $P_{ox}$  and increasing rate. This confirms that the growth rate predominantly affects the oxy-

gen content, rather than the density of extended structural defects (dislocations, twins, and low-angle grain boundaries), which may also change with rate.<sup>22</sup>

While pure TiO<sub>2</sub> films grown at 5 Hz and  $7 \times 10^{-5}$  mbar show typical semiconductor behavior with freezing out of the carriers at low  $T$ , the Co-doped films grown under identical conditions display different behavior (pink symbols in Fig. 2, bottom panel). The Hall constant is orders of magnitude smaller and exhibits a clear maximum at around 100 K, after which  $R_H$  goes down and approaches a constant value at low  $T$ . Similar behavior was found for a variety of Co:TiO<sub>2</sub> films with thickness between 75 and 550 nm grown at oxygen pressure between  $7 \times 10^{-5}$  and  $3 \times 10^{-3}$  mbar, while at  $6 \times 10^{-3}$  mbar, the maximum in  $R_H$  has shifted to above room temperature (Fig. 2, bottom panel). The Hall constant at low  $T$  is remarkably insensitive to the growth conditions, approaching a value of  $0.5\text{--}1 \text{ cm}^3/\text{C}$  for all films, corresponding to  $n=6 \times 10^{18}\text{--}1.2 \times 10^{19} \text{ cm}^{-3}$ .

Similar behavior with a maximum in  $R_H$  was previously found in other highly doped (nonmagnetic) semiconductors such as Ge, and it is well established that this is due to a competition between two conduction processes,<sup>15,23</sup> at high  $T$ , transport is by conduction band electrons thermally excited from shallow donors, while at low  $T$ , a transition occurs to transport dominated by a donor-derived impurity band. The maximum in  $R_H$  and the saturation at low  $T$  are the hallmark features of *metallic* impurity conduction.<sup>15</sup> The relatively large  $r_H$  in the anatase phase of Co:TiO<sub>2</sub> allows impurity band conduction at rather low carrier density.<sup>21</sup> Note that the carrier concentration of about  $6 \times 10^{18} \text{ cm}^{-3}$  is a factor of 70 smaller than the Co cation concentration ( $4.1 \times 10^{20} \text{ cm}^{-3}$  for 1.4% of Co). Since Co is consistently found<sup>7,24–27</sup> in a Co<sup>2+</sup> state in Co:TiO<sub>2</sub>, the substitution of Ti<sup>4+</sup> by Co<sup>2+</sup> requires transfer of two electrons from nearby oxygen and the creation of an oxygen vacancy. In such ionic picture, the two electrons are bound to the Co. However, free carriers can result from hybridization between the magnetic cation states and the shallow donor levels.<sup>12,28</sup> To obtain the observed carrier concentration of about 1% of the Co cation concentration, one would require only a very small deviation from a purely Co<sup>2+</sup> state, consistent with experiments.<sup>7,24–27</sup> However, a somewhat larger deviation plus compensation by other impurities and/or defects can also yield the observed carrier concentration.

The maximum in  $R_H$  is described by a phenomenological two-band transport model<sup>15</sup> in which the conductivity is the sum of a contribution  $\sigma_{cb}(T)=n_{cb}(T)e\mu_{cb}(T)$  from electrons thermally excited into the conduction band and a contribution from impurity band conduction  $\sigma_{ib}(T)=n_{ib}(T)e\mu_{ib}(T)$ , with  $\mu_{cb,ib}$  the respective mobility. For the carrier density, a fraction  $n_{cb}(T)=n_0 \exp(-E_A/k_B T)$  of the total number of carriers  $n_0$  is excited into the conduction band (activation energy  $E_A$ ,  $k_B$  is the Boltzmann constant). The remaining electrons reside in the impurity band:  $n_{ib}(T)=n_0-n_{cb}(T)$ . The total Hall constant can then be calculated<sup>15</sup> and exhibits a maximum at a temperature  $T_{max}^{Hall}$  that is controlled mainly by  $\mu_{ib}$  and  $E_A$ . As shown by the fits in the inset of Fig. 2, bottom panel, the model describes the Hall data well. The correct position of the maximum of the Hall constant is obtained for

$E_A$  of about 30 meV (colored solid line), although the predicted transition is more sharp and the data deviate on the low  $T$  side. The fit is improved by adding a small amount ( $\approx 1\%$ ) of carriers with a lower activation energy (black solid line). The significant improvement for such a rather small number of carriers with lower activation energy is due to the combined effect of (i) the exponential dependence of  $n_{cb}(T)$  on the activation energy, causing these carriers to be excited into the conduction band at lower temperature, (ii) the larger mobility  $\mu_{cb}(T)$  for these carriers at low  $T$  because of the reduced phonon scattering, resulting in a comparatively large contribution to the conduction, and (iii) the inverse relation between Hall voltage and carrier density, such that a small number of carriers produce a large Hall voltage. At higher  $T$ , conduction is again dominated by the larger number of carriers with the higher activation energy, and hence the fit is not affected much in this regime.

The temperatures at which the maximum of the Hall constant ( $T_{max}^{Hall}$ ) and the mobility ( $T_{max}^{mob}$ ) occur show a systematic trend upon changing  $P_{ox}$  (Fig. 3, bottom panels). Parenthetically, the doped and undoped films behave oppositely. When  $P_{ox}$  is larger,  $T_{max}^{Hall}$  decreases for undoped films, while it increases for the Co-doped films. Moreover,  $T_{max}^{mob}$  remains at around 120 K for all undoped films, while  $T_{max}^{mob}$  is shifted to higher  $T$  for Co-doped films grown at larger  $P_{ox}$ . The undoped films behave as expected. At high  $P_{ox}$ , there are few shallow donors and the conductivity is dominated by  $\sigma_{cb}$ . When  $P_{ox}$  is reduced, the number of shallow donors increases, and thereby  $\mu_{ib}$  increases. This shifts  $T_{max}^{Hall}$  to higher  $T$ . Nevertheless, for  $E_A \sim 20$  meV, the calculated Hall maximum is only at 65 K even for reasonably large  $\mu_{ib}$  of  $\sim 2 \text{ cm}^2/\text{V s}$ , such that conduction band electrons still dominate for  $T > 65$  K. Hence,  $T_{max}^{mob}$  remains unchanged at 110 K.

Evidently, the opposite behavior of Co:TiO<sub>2</sub> cannot be explained in a similar way. We thus examine the other parameter ( $E_A$ ) that controls the relative weight of the two conduction channels. A larger  $E_A$  exponentially suppresses  $\sigma_{cb}$  and thereby shifts  $T_{max}^{Hall}$  and  $T_{max}^{mob}$  to higher values. Qualitative agreement with the experimental trend is obtained when  $E_A$  varies from  $\sim 30$  meV to beyond  $\sim 70$  meV as  $P_{ox}$  increases. The data suggest that for films grown under more oxygen poor conditions, the Fermi level shifts toward the conduction band. Perhaps coincidental, these electronic changes are accompanied by stronger ferromagnetism for growth at lower  $P_{ox}$  (Fig. 3, top panel). Films grown at  $P_{ox}$  of  $7 \times 10^{-5}$  mbar are ferromagnetic at room temperature having a nonzero remanence and a coercivity of about 300 Oe. Films grown at higher  $P_{ox}$  have reduced magnetic moments, while the remanence and coercivity disappear for films grown at  $P_{ox}$  of  $10^{-3}$  mbar.

Direct evidence for the interaction between Co spins and mobile carriers comes from the Kondo effect. In normal metals with randomly dispersed dilute magnetic impurities, this is manifested as a minimum in the  $\rho$  versus  $T$  curve, followed by a characteristic logarithmic increase of  $\rho$  at low  $T$ . Unlike metals, in semiconductors,  $n$  varies with  $T$ , which can easily mask the Kondo effect in the resistivity. Since

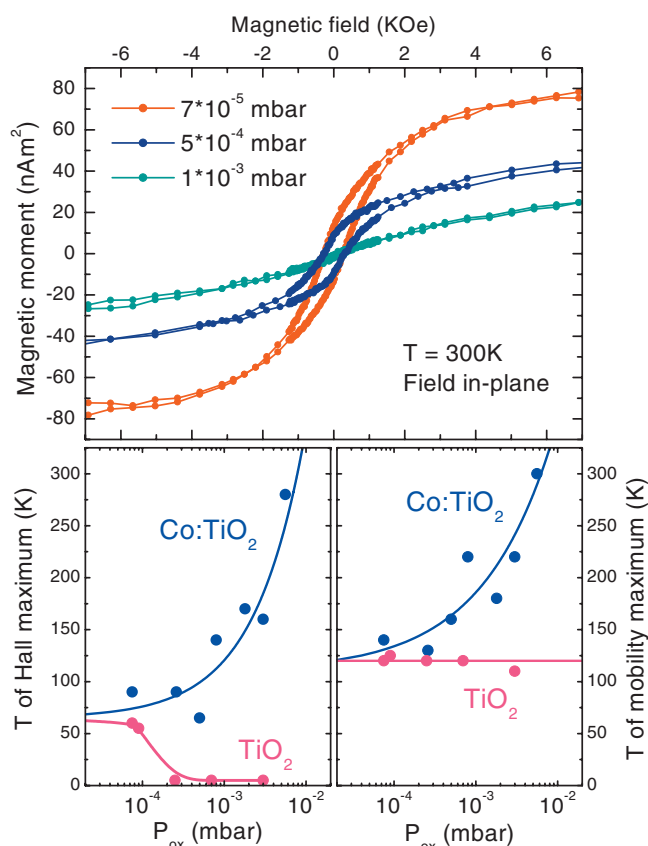


FIG. 3. (Color) Top panel: magnetic moment versus in-plane applied field for Co:TiO<sub>2</sub> films grown at different  $P_{ox}$ . Bottom panels: variation of  $T_{max}^{Hall}$  (left) and  $T_{max}^{mob}$  (right) versus  $P_{ox}$ , with the laser repetition rate kept constant. Pink symbols are for undoped anatase TiO<sub>2</sub>; blue symbols are for Co:TiO<sub>2</sub>. Solid lines are a guide to the eyes.

$\rho = 1/ne\mu$ , we instead plot  $1/\mu$  versus  $T$  (Fig. 4, inset). We observe a pronounced minimum and an increase at low  $T$  that follows a logarithmic dependence, consistent with Kondo scattering of the conduction electrons. Extrapolation to the horizontal axis defines Kondo temperatures  $T_K$  of 60 and 120 K, respectively, for the two films shown in the inset. The main panel of Fig. 4 shows data as a function of reduced temperature  $T/T_K$ , showing scaling with data collapsing onto a single curve for several Co:TiO<sub>2</sub> films with different  $T_K$ . From transport analysis (Fig. 2), we know that conduction is dominated by the metallic impurity band in the logarithmic regime below about 100 K. Therefore, the Kondo effect is attributed to the resonant scattering of the electrons at the Fermi level in the metallic impurity band. Weak localization can be ruled out as this requires two dimensional transport to produce a logarithmic  $T$  dependence, while our transport is clearly three dimensional as films have thickness (150–200 nm) much larger than the mean free path (of the order of a few nanometers). We did not find the logarithmic behavior in any of the pure TiO<sub>2</sub> films, identifying Co local spins as the scattering centers. We note that the nominal Co content is higher than the carrier concentration. However, it is not unlikely<sup>9,26</sup> that the Co distribution is not homogeneous and that only a small fraction of the Co exists as iso-

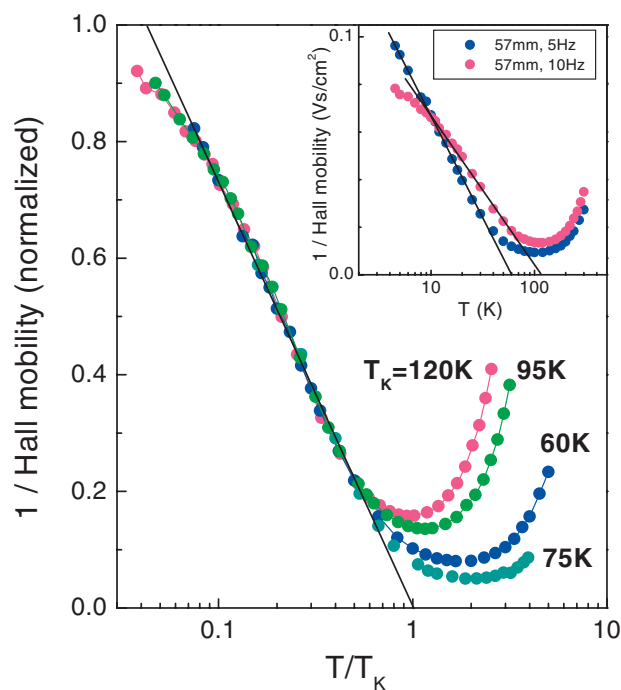


FIG. 4. (Color) Kondo effect in Co:TiO<sub>2</sub>, shown as the inverse of the Hall mobility versus temperature normalized to  $T_K$ . The vertical scale is normalized to have a value of 0.5 at  $T/T_K = 0.2$  for each curve. All films are grown at  $9 \times 10^{-5}$  mbar. Target-substrate distance and laser repetition rate are, respectively, 57 mm and 10 Hz ( $T_K = 120$  K), 57 mm and 5 Hz ( $T_K = 60$  K), 48 mm and 5 Hz ( $T_K = 75$  K), and 48 mm and 10 Hz ( $T_K = 95$  K). The inset shows data without normalization for the two films grown at 57 mm.

lated spins. In fact, this is similar to GaMnAs, where Kondo effects due to a small fraction of Mn *interstitials* were recently reported,<sup>29</sup> albeit with  $T_K$  below 10 K. Values of  $T_K$  up to 120 K observed here for anatase Co:TiO<sub>2</sub> are remarkably high and about an order of magnitude higher than typically observed in metals. This suggests a strong interaction between Co spins and conduction electrons in the impurity band and implies that conduction electrons and the Co local moments are in states that are energetically sufficiently close to produce strong interaction. The Kondo effect provides an avenue to study interactions between carriers and local spins in a variety of oxide magnetic semiconductors that have mobile carriers. The origin of the high Kondo temperature and the relation, if any, to the high magnetic ordering temperatures in oxide FMSC are to be further explored. Moreover, being a many body effect, the observation of the Kondo effect in a magnetic semiconductor suggests that theoretical descriptions of oxide FMSC have to go beyond the single particle models that have so far been unable to explain the unusually high magnetic ordering temperatures.

We thank D. H. A. Blank and A. J. H. M. Rijnders for the PLD facilities and acknowledge financial support from the NWO-VIDI program and the NanoNed and NanoImpuls programs coordinated by the Dutch Ministry of Economic Affairs.

- <sup>1</sup>H. Ohno, *Science* **281**, 951 (1998).
- <sup>2</sup>T. Dietl, H. Ohno, F. Matsukura, J. Cibert, and D. Ferrand, *Science* **287**, 1019 (2000).
- <sup>3</sup>H. Ohno, D. Chiba, F. Matsukura, T. Omiya, E. Abe, T. Dietl, Y. Ohno, and K. Ohtani, *Nature (London)* **408**, 944 (2000); D. Chiba, M. Yamanouchi, F. Matsukura, and H. Ohno, *Science* **301**, 943 (2003).
- <sup>4</sup>S. A. Wolf, D. D. Awschalom, R. A. Buhrman, J. M. Daughton, S. von Molnár, M. L. Roukes, A. Y. Chtchelkanova, and D. M. Treger, *Science* **294**, 1488 (2001).
- <sup>5</sup>Y. Matsumoto, M. Murakami, T. Shono, T. Hasegawa, T. Fukumura, M. Kawasaki, P. Ahmet, T. Chikyow, S.-Y. Koshihara, and H. Koinuma, *Science* **291**, 854 (2001).
- <sup>6</sup>Y. Matsumoto, R. Takahashi, M. Murakami, T. Koida, X.-J. Fan, T. Hasegawa, T. Fukumura, M. Kawasaki, S.-Y. Koshihara, and H. Koinuma, *Jpn. J. Appl. Phys., Part 2* **40**, L1204 (2001).
- <sup>7</sup>S. A. Chambers, S. Thevuthasan, R. F. C. Farrow, R. F. Marks, J. U. Thiele, L. Folks, M. G. Samant, A. J. Kellock, N. Ruzycski, D. L. Ederer, and U. Diebold, *Appl. Phys. Lett.* **79**, 3467 (2001).
- <sup>8</sup>H. Toyosaki, T. Fukumura, Y. Yamada, K. Nakajima, T. Chikyow, T. Hasegawa, H. Koinuma, and M. Kawasaki, *Nat. Mater.* **3**, 221 (2004).
- <sup>9</sup>S. A. Chambers, C. M. Wang, S. Thevuthasan, T. Droubay, D. E. McCready, A. S. Lea, V. Shutthanandan, and C. F. Windisch, Jr., *Thin Solid Films* **418**, 197 (2002).
- <sup>10</sup>K. Ueda, H. Tabata, and T. Kawai, *Appl. Phys. Lett.* **79**, 988 (2001).
- <sup>11</sup>S. B. Ogale, R. J. Choudhary, J. P. Buban, S. E. Lofland, S. R. Shinde, S. N. Kale, V. N. Kulkarni, J. Higgins, C. Lanci, J. R. Simpson, N. D. Browning, S. Das Sarma, H. D. Drew, R. L. Greene, and T. Venkatesan, *Phys. Rev. Lett.* **91**, 077205 (2003).
- <sup>12</sup>J. M. D. Coey, M. Venkatesan, and C. D. Fitzgerald, *Nat. Mater.* **4**, 173 (2005).
- <sup>13</sup>J. Philip, A. Punnoose, B. I. Kim, K. M. Reddy, S. Layne, J. O. Holmes, B. Satpati, P. R. LeClair, T. S. Santos, and J. S. Moodera, *Nat. Mater.* **5**, 298 (2006).
- <sup>14</sup>S. R. Shinde, S. B. Ogale, S. Das Sarma, J. R. Simpson, H. D. Drew, S. E. Lofland, C. Lanci, J. P. Buban, N. D. Browning, V. N. Kulkarni, J. Higgins, R. P. Sharma, R. L. Greene, and T. Venkatesan, *Phys. Rev. B* **67**, 115211 (2003).
- <sup>15</sup>N. F. Mott and W. D. Twose, *Adv. Phys.* **10**, 107 (1961).
- <sup>16</sup>K. S. Burch, D. B. Shrekenhamer, E. J. Singley, J. Stephens, B. L. Sheu, R. K. Kawakami, P. Schiffer, N. Samarth, D. D. Awschalom, and D. N. Basov, *Phys. Rev. Lett.* **97**, 087208 (2006).
- <sup>17</sup>A. C. Hewson, *The Kondo Problem to Heavy Fermions* (Cambridge University Press, Cambridge, 1993).
- <sup>18</sup>S. M. Cronenwett, T. H. Oosterkamp, and L. P. Kouwenhoven, *Science* **281**, 540 (1998).
- <sup>19</sup>R. Ramaneti, J. C. Lodder, and R. Jansen, *Appl. Phys. Lett.* **91**, 012502 (2007).
- <sup>20</sup>R. J. Kennedy, P. A. Stampe, E. Hu, P. Xiong, S. von Molnár, and Y. Xin, *Appl. Phys. Lett.* **84**, 2832 (2004).
- <sup>21</sup>H. Tang, K. Prasad, R. Sanjines, P. E. Schmid, and F. Levy, *J. Appl. Phys.* **75**, 2042 (1994).
- <sup>22</sup>T. C. Kaspar, S. M. Heald, C. M. Wang, J. D. Bryan, T. Droubay, V. Shutthanandan, S. Thevuthasan, D. E. McCready, A. J. Kellock, D. R. Gamelin, and S. A. Chambers, *Phys. Rev. Lett.* **95**, 217203 (2005).
- <sup>23</sup>H. Fritzsche and M. Cuevas, *Phys. Rev.* **119**, 1238 (1960).
- <sup>24</sup>K. A. Griffin, A. B. Pakhomov, C. M. Wang, S. M. Heald, and K. M. Krishnan, *Phys. Rev. Lett.* **94**, 157204 (2005).
- <sup>25</sup>S. A. Chambers, S. M. Heald, and T. Droubay, *Phys. Rev. B* **67**, 100401(R) (2003).
- <sup>26</sup>J.-Y. Kim, J.-H. Park, B.-G. Park, H.-J. Noh, S.-J. Oh, J. S. Yang, D.-H. Kim, S. D. Bu, T.-W. Noh, H.-J. Lin, H.-H. Hsieh, and C. T. Chen, *Phys. Rev. Lett.* **90**, 017401 (2003).
- <sup>27</sup>J. D. Bryan, S. M. Heald, S. A. Chambers, and D. R. Gamelin, *J. Am. Chem. Soc.* **126**, 11640 (2004).
- <sup>28</sup>K. R. Kittilstved, W. K. Liu, and D. R. Gamelin, *Nat. Mater.* **5**, 291 (2006).
- <sup>29</sup>H. T. He, C. L. Yang, W. K. Ge, J. N. Wang, X. Dai, and Y. Q. Wang, *Appl. Phys. Lett.* **87**, 162506 (2005).